CHAPTER 2

THEORETICAL BACKGROUND

The understanding of standard trapping and cooling techniques is necessary in preparing the cold atoms. This chapter begins by reviewing a fundamental physics that underlines these techniques in Section 2.1. After the atoms are trapped, the loss due to the cold collisions induced by laser light is considered; the detail is discussed in Section 2.2.

2.1 Cooling and trapping for neutral atoms

For the reason that atoms normally at room temperature must be cooled down before they can be captured and trapped, the basic of cooling mechanism such as Doppler cooling is introduced first in Section 2.1.1. In Section 2.1.2 a widely used Magneto-optical trap (MOT) is presented. The MOT is a combination of the Doppler cooling and an inhomogeneous quadrupole magnetic field. This technique exploits the Zeeman splitting to further enhance the trapping mechanism greatly [28]. Another kind of trap used in this study is an optical dipole trap explained in Section 2.1.3. It is based on the interaction between the electric-dipole moment of the atoms and the electric field of light. In this thesis, a polarization gradient cooling and a Sisyphus cooling were also used for further decreasing the kinetic energy of the trapped atoms. These cooling techniques are detailed in Section 2.1.4 and Section 2.1.5 respectively.

2.1.1 Doppler cooling

In the laser cooling theory, the temperature of an atomic ensemble T is defined by using an average of the atomic kinetic energy $\langle E_k \rangle$ in one dimension [29]:

$$\frac{1}{2} k_B T = \langle E_k \rangle. \tag{2.1}$$

This temperature assignment is adequate for the atoms that are in thermal equilibrium. At the equilibrium, the atomic velocity distribution is assumed to be the Mazwell-Boltmann (MB) distribution, which only depends on the speed of the atoms given by

$$f(v) = \sqrt{\frac{m}{2\pi k_B T}} \exp\left(-\frac{mv^2}{2k_B T}\right), \tag{2.2}$$

where m is an atomic mass and v is an atomic speed in one dimension.

As mentioned above, when an atom is cold, it moves slowly. On the other hand, a worm atom moves very quickly. Since the velocity distribution of the atoms is directly related to their temperature. The idea of Doppler cooling is to slow down these atoms by applying the laser light while the Doppler effect plays a crucial role as following details.

The capability of laser light to slow down atoms comes from the momentum transfer from the photons in the light beam to the atoms. To understand this, let us consider the system of an atom at rest interacting with a laser beam, of which the frequency is ω_0 resonant with an atom transition as shown in Figure 2.1. The atom may absorb the photon and change its state from the ground state to the excited state.

Then it emits a photon spontaneously in a random direction and goes back to the ground state.

After n absorption/emission cycles a total momentum transfer to the atom due to the absorptions (n photons) is equal to $n\hbar\mathbf{k}$ in the same direction of the laser as represented by the pink arrow, where $\mathbf{k}$ is the wave vector of incident photons. The total momentum transfer due to the spontaneous emissions is zero due to the random direction of the emitted photons. As a result, the net momentum transfer to the atom is $n\hbar\mathbf{k}$ as represented by the green arrow. From these momentum exchanges, the

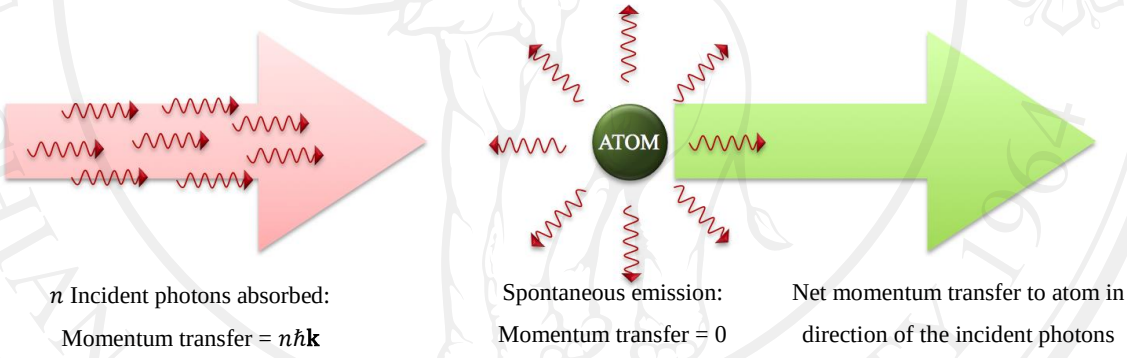

Figure 2.1. Momentum transfer in the laser cooling process. An atom at rest in laser beam absorbs a photon (represented by the small red arrow) in the incident laser beam, and then emits a photon spontaneously.

Figure 2.2. The Doppler effect in the laser cooling process in one dimension. The details are described in text.

atom experience a force called “the radiative force” with a corresponding time-averaged acceleration of [30]:

$$\langle \vec{a} \rangle = \frac{\hbar \mathbf{k} R(I,\omega)}{m}, \tag{2.3}$$

where $R(I,\omega)$ is the absorption rate which depend on the light intensity I and the light frequency ω. For a stationary atom in space, the absorption rate can be calculated to be:

$$R(I,\omega) = \frac{\Gamma}{2} \frac{I/I_s}{1 + I/I_s + (2(\omega - \omega_0)/\Gamma)^2}, \tag{2.4}$$

where Γ is the natural line width of an atomic transition and I_s is the saturation intensity. From this equation, the atom has the maximum absorption rate when the light frequency is ω_0.

However, an atom has non-zero velocity. Thus the Doppler effect must be taken into accounted. As shown in Figure 2.2 when the atom counter propagates the light beam at a specific speed v, it experiences an increase in the light frequency amounted to $(v/c)\omega$, where ω is the light frequency in the rest frame and c is the speed of light. For this matter, if the laser beam is red detuned ($\omega < \omega_0$) from the resonance frequency of the atom, the atom can experience a light frequency shifted up to nearly ω_0. This leads to the atom having absorbed more photons with high $R(I,\omega)$ from the light beam. The opposite is also true when the atom moves along in the same direction of the beam.

The counter-propagating red-detuned laser beams are used for slowing down or cooling down the atom. The radiative force of the beam moving toward the atom is larger than that from the opposite direction as explained above. The velocity of the atom either the direction of the laser beams is decreased. To extend this cooling technique into three dimensions, we use three pairs along three mutually orthogonal axes in three dimensions. The atomic cloud is slowed down within the overlapping volume where the beams intersected. This essentially produces velocity-dependent damping force analogous to when a particle travels in sugar molasses and thus name the "optical molasses".

However, the heating due to the stochastic nature of photon absorption and emission leads to the limit of this cooling technique. At a low-intensity and the red detuning equal to $\Gamma/2$, the minimum limit of this Doppler temperature [30] is

$$T_D = \frac{\hbar\Gamma}{2k_B}. \tag{2.5}$$

This limit is typically several hundred μK. Associated with this temperature is the velocity in one dimension $v_D = \sqrt{k_B T/m}$.

2.1.2 Magneto-optical trap

In the optical molasses the atoms are not trapped and as a result a position dependent force is needed. We may introduce this force by applying a linearly inhomogeneous magnetic field to our atomic sample. This will create a broken symmetry that lifts

degeneracy of all magnetic sublevels in the atoms, recognized as the Zeeman splitting or the Zeeman effect [31].

Let us consider an atom with a ground state $J = 0$ and an excited state $J' = 1$ in the magnetic field $\mathbf{B} = B_z\hat{z}$ where B_z is directly proportional to z as shown in Figure 2.3. The counter-propagated light beams with right-handed (σ_+) and left-handed (σ_-) polarizations red detuned by δ from the zero field atomic resonance are applied as indicated by the red arrows. The energy of the atomic states shifts proportional to $m_j B_z$ as a result of Zeeman effect. In the right hand side, the excited state with quantum number $m_1 = +1$ is shifted up due to $B_z > 0$ where the state $m_1 = -1$ is shifted down. Suppose that the atom is at position z'. The detuning of the light from the $\Delta m = -1$ atomic transition (from the ground state with $m_0 = 0$ to the excited state with $m_1 = -1$) is small as indicated by δ_- in the figure but the detuning from the $\Delta m = +1$ transition indicated by δ_+ is much larger than the other one. Due to the selection rules for circularly polarized light, the $\Delta m = -1$ and $\Delta m = +1$ transitions can occur only by absorbing the σ_- light and the σ_+ light respectively [30]. Thus the atom interacts more with the radiative force by the σ_- light than by the σ_+ one. As a result, it is pushed toward the origin where the magnetic field vanishes. On the other side ($B_z < 0$), the atom interacts more with the σ_+ light and again the atom is pushed toward the center.

This effect operates in position space to confine and push atoms back to the center of the trap, whereas the optical molasses mentioned before operate in velocity space to slow down the atoms. This technique operating in both position and velocity space is called Magneto-optical trap (MOT).

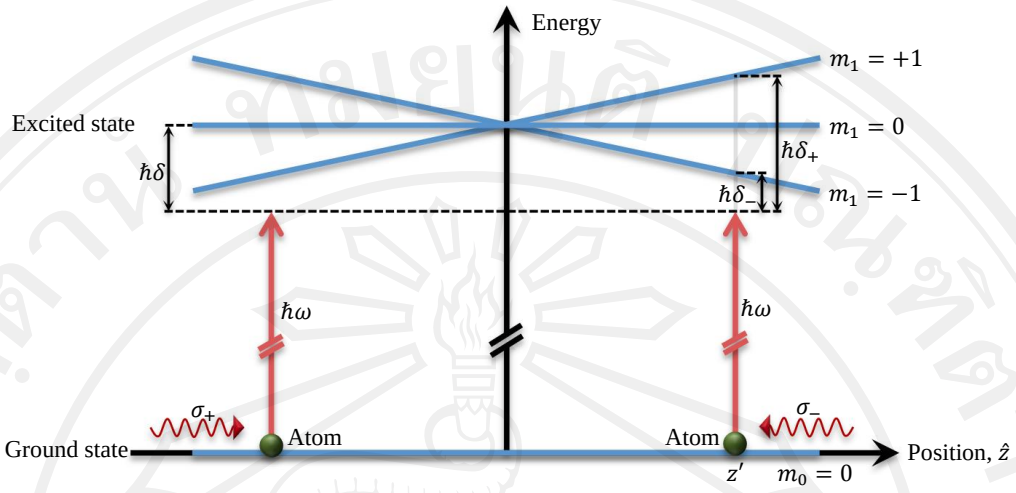

Figure 2.3. Cooling mechanism in one-dimensional MOT. The atomic ground state and first excited state are indicated by the total angular momentum of $\boldsymbol{J = 0}$ and $\boldsymbol{J' = 1}$ respectively. The excited state is split because of the Zeeman effect.

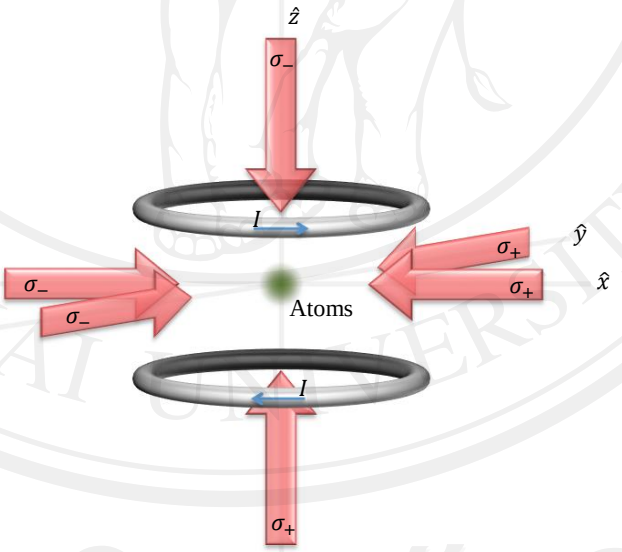

Figure 2.4. Schematic of the MOT. Six lasers beams are shined as represented by the red arrows. The directions of the current $\boldsymbol{I}$ applying to the anti Helmholtz coils are indicated by blue arrows.

The configuration of the MOT is shown in Figure 2.4. Three pairs of counter-propagating light beam have the circular polarization as described above. The overlapping region of the beams is aligned at the center of a quadrupole magnetic field. The field is created by using two coils in anti-Helmholtz configuration for which current in each coil runs in opposite direction. A MOT cloud of atoms is accumulated in this region.

2.1.3 Dipole traps

In this study, the cold MOT atoms were loaded into an optical dipole trap to study their properties and their collision process. (By loading into the dipole trap, a compressed MOT (cMOT) [30], following with the optical molasses as described in Section 2.1.4, were performed.) The advantages for using the dipole traps are: the atoms in dipole traps have much lower interaction with the trapping light compared with the MOT configuration; the trap depth can be adjusted conveniently by changing the power of the trapping laser; and the dipole traps can be scalable conveniently.

The crucial key of the dipole traps is that the energy level of the atoms is shifted when an atom interacts with a light field. The gradient of the energy can create a confining dipole force for the atoms. The concepts of atom interacting with the field can be explained by using a dressed state pictures that treat a quantized atom interacting with a quantized light field. First, the optical trap is described by considering two-level atoms before the behavior of real multilevel atoms is exposed at the end.

Atoms in a quantized light field

In a quantum mechanical picture, an interaction of a quantized atom with a quantized monochromatic single mode laser field is treated and the eigenstates of this system are "dressed states". The corresponding eigenenergies are shifted as a function of the detuning and the number of photons in the field. This system treatment starts from the two level atom and then extends to all possible transition states.

Let us start with the uncoupled Hamiltonian, which is the sum of two parts: $H_0 = H_A + H_L$, where H_A is the atomic Hamiltonian and H_L is the Hamiltonian of the laser field. H_A can be taken from the sum of a kinetic energy of an atom and an atomic internal energy. However in this treatment, the kinetic energy term is omitted [32] and H_A is then

$$H_A = \hbar\omega_0 b^+ b. \tag{2.6}$$

Here $b^+ = |e\rangle\langle g|$ and $b = |g\rangle\langle e|$ are the raising and lowering operators respectively, where $|g\rangle$ is an atomic ground state with zero energy and $|e\rangle$ is an excited one with energy $\hbar\omega_0$. For the laser mode containing photon of energy $\hbar\omega$, the Hamiltonian of this single mode quantized field is

$$H_L = \hbar\omega(a^+ a + \frac{1}{2}), \tag{2.7}$$

where a^+ and a are the creation and annihilation operator respectively.

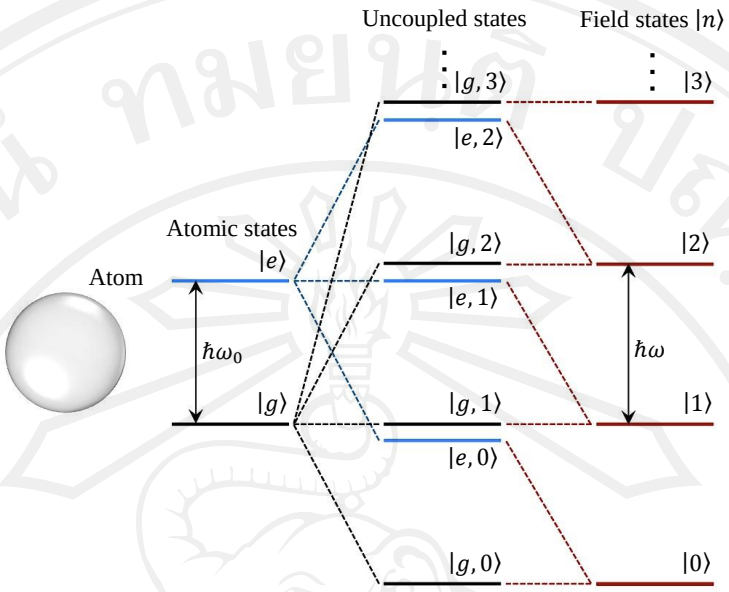

Figure 2.5. Energy level scheme for the atom with the $|g\rangle$ and $|e\rangle$ states (left) and the atom plus field Hamiltonian of uncoupled system.

An energy diagram of uncoupled system H_0 is shown in Figure 2.5. The ordinary atomic state levels ($|g\rangle$ and $|e\rangle$) are repeated for each photon number n and are shifted up by $\hbar\omega$ (the energy of the photon in the field). Then the attention is focused into the two closed adjacent levels of $|g, n+1\rangle$ and $|e, n\rangle$ called manifolds. In each manifold, the levels are spaced by $\hbar\omega_0 - \hbar\omega = \hbar\delta$ where δ is the detuning of the laser.

For atom-laser photon coupling, the interaction between the atomic dipole and the laser field is represented by

$$H_{AL} = -\mathbf{d} \cdot \mathbf{E}(\mathbf{r}) = k(b^{+}a + ba^{+}), \tag{2.8}$$

where $\mathbf{d} = \mathbf{d}_{ge}(b^+ + b)$ is atomic electric-dipole moment operator ($\mathbf{d}_{ge} = \langle g|\mathbf{d}|e\rangle = \langle e|\mathbf{d}|g\rangle$), $\mathbf{E(r)} = \mathbf{e}\sqrt{\frac{\hbar\omega}{2\epsilon_0 V}}(a + a^+)$ is the laser field operator with a classical atomic position $\mathbf{r}$ (where $\mathbf{e}$ is the unit polarization vector and V is the volume of the field cavity), and k is a coupling constant equal to $-\mathbf{e}\cdot\mathbf{d}_{ge}\sqrt{\frac{\hbar\omega}{2\epsilon_0 V}}$ [33]. This coupling H_{AL} represents the excitation (first term) and stimulated emission (second term) of the atom induced by the light field. When the atom-laser coupling is taken into account, the dressed-atom Hamiltonian is

$$H_{DA} = H_0 + H_{AL} \tag{2.9}$$

and the new eigenstates called "dressed states" are

$$|1, n\rangle = \sin\theta|g, n+1\rangle + \cos\theta|e, n\rangle$$

$$|2, n\rangle = \cos\theta|g, n+1\rangle - \sin\theta|e, n\rangle, \tag{2.10}$$

where the angle θ is define by $\tan 2\theta = -\Omega/\delta$ and $0 \leq \theta \leq \pi$. Here Ω is Rabi frequency, which is equal to $\frac{2}{\hbar}k\sqrt{\langle n\rangle}$ [33].

From the coupling, the energy levels of the dressed states are shifted from the uncoupled ones by ΔE as shown in Figure 2.6. The separation of each pair of dressed states is calculated by an interval

$$\hbar\Omega' = \hbar\sqrt{\delta^2 + \Omega^2} \tag{2.11}$$

and are symmetry located with respect to the uncoupling ones.

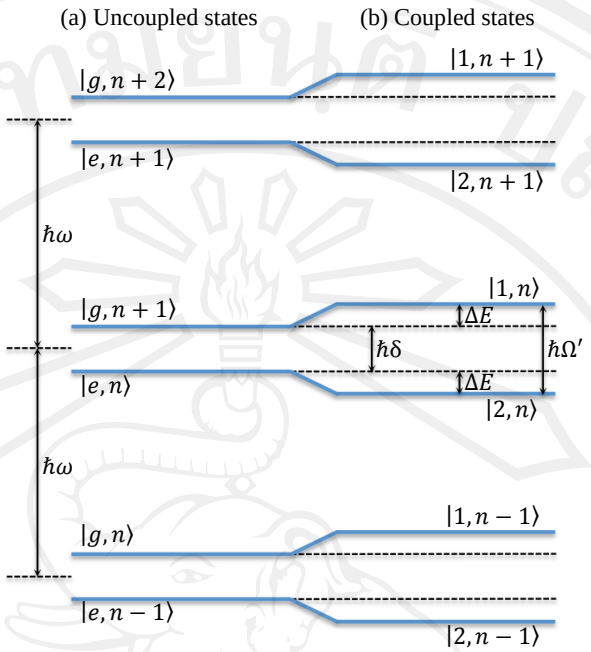

Figure 2.6. Dressed-atom energy diagram that shows uncoupled states in (a) and coupled states in (b) of the states combined atom-laser mode system.

The value of ΔE represented in Figure 2.6 (b) is equal to $\Delta E = \frac{\hbar}{2}(\Omega' - \delta)$. Let us consider in the case of far detuning ($\delta \gg \Omega$). Then ΔE can be approximated by :

$$\Delta E = \pm \frac{\hbar \Omega^2}{4\delta}. \tag{2.12}$$

The upper and lower sign are applied for the ground and excited states respectively.

Consider an atomic transition from a ground state with angular momentum J to an excited state with angular momentum J'. For this real multilevel atom, its energy shifts depend on the hyperfine states and can be expressed using a real transition coefficient or "Clebsch-Gordan coefficient, C_{ij}" and a reduced matrix element $\langle J' | \mathbf{d} | J \rangle$. If $|g_i\rangle$ and $|e_j\rangle$ are the considered states and $\langle g_i | \mathbf{d} | e_j \rangle = C_{ij} \langle J' | \mathbf{d} | J \rangle$,

the energy shift of specific state $|g_i\rangle$ can be calculated by summing up the contributions of all coupled excited states $|e_j\rangle$:

$$\Delta E_i = \frac{\hbar\Omega^2}{4}\sum_j \frac{C_{ij}^2}{\delta_{ij}}, \tag{2.13}$$

where δ_{ij} is the detuning of the laser field of the transition from $|g_i\rangle$ to $|e_j\rangle$.

The optically induced shift of the atomic energy level is known as the "light shift" or "ac Stark shift". The light shift of the ground state ΔE_i exactly corresponds to the dipole potential $U_{dip,i}$ that can be used for trapping atoms.

Dipole trap realization

To create the optical trap, a specific frequency light is used. From the state-dependent ground-state dipole potential, two specific types of real experiments are described in detail in the subsection below. As seen in the equation (2.13) the shifted energy of atom is directly proportional to the number of photon but inversely proportional to the laser detuning. If the light is red detuned ($\delta < 0$), the shifted energy has a negative value. In consequence the atom is attracted to the highest light intensity (or highest number of photons) region where the energy level of the atom is lowest. In the opposite if the light is blue detuned ($\delta > 0$), the atoms can be accumulated at the lowest light intensity region.

To create the trap, the repulsive blue-detuned light has to be applied surrounding the atoms as illustrated in Figure 2.7 (right). The atoms are trapped in the dark place leading to the great advantage of this kind of trap. The trapped atoms

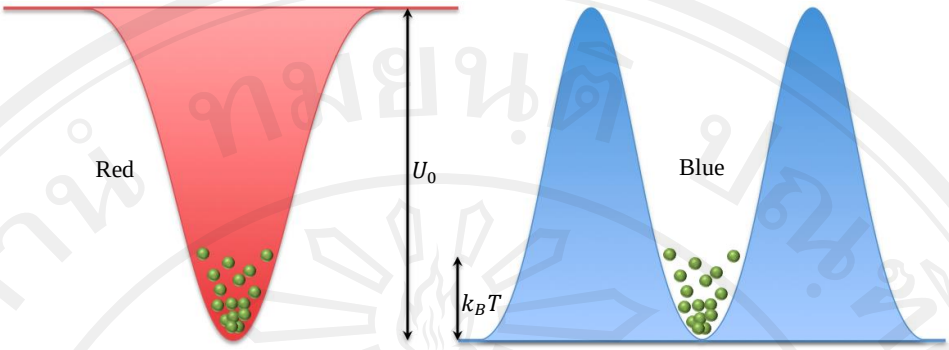

Figure 2.7. The cold atoms with temperature $\boldsymbol{T}$ trapped in the $\boldsymbol{U_0}$ deep optical traps using red (left figure) or blue (right figure) detuned light.

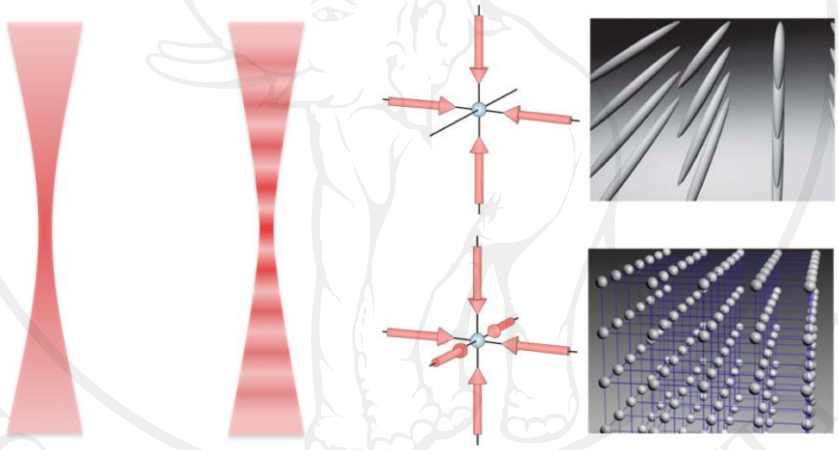

(a) (b) (c)

Figure 2.8. Red detuned light beam configurations for far-off resonance trap (FORT). (a) Focused-beam trap: the Gaussian beam is focused to create gradient of intensity in the axial axis of the beam. (b) Standing-wave trap: the counter propagating focused-beams create the one-dimensional optical trapping array. (c) Crossed-beam trap: two (top figure) or three pairs (bottom figure) of the counter propagating focused-beams are crossed each to create a two-dimensional or a three-dimensional trapping array, respectively [38].

are little affected by photon scattering, collisional losses induced by the light, and the light shifts of the atomic energy level. However, the blue-detuned trap is not simple to be realized. To create the optical walls, the three mains methods have been purposed that are the light sheets [34], the hollow laser beams [35], and Evanescent waves [36].

For a red detuned dipole trap, atoms are trapped where a light intensity is greatest as illustrated in Figure 2.7 (left). Experimentally the optical potential is easily generated using the focus of a far-red-detuned Gaussian beam (illustrated in Figure 2.8 (a)) that is called far-off resonance trap or FORT [37].

An optical dipole trap is scalable conveniently. In Figure 2.8 (b), a one-dimensional optical trapping array can be straightforwardly generated from a pair of the counter propagating red detuned focused-beams. The atoms can be axially confined at the antinodes of the standing wave. An addition of more laser beams to the 1D configuration leads to a two-dimensional or three-dimensional optical array as shown in Figure 2.8 (c); the two (top) or three (bottom) pairs of orthogonal standing wave are intersected at their foci where the 2D or 3D trapping array are created.

In our study, the cold atoms were loaded into FORT, of which more details are explained in Chapter 4. As the FORT has no cooling mechanism, it is necessary to apply others cooling light beams for reducing the excess kinetic energy of the trapped atoms that make the atoms stay in the trap longer. For example, the polarization gradient cooling was used (Section 2.1.4) during the collision duration and the Sisyphus cooling was formed (Section 2.1.5) during the imaging duration. The theories of both cooling techniques are explained below.

2.1.4 σ_--σ_+ polarization gradient cooling

The Doppler cooling theory described before neglects the degeneracies of atomic energy levels. Atoms that are moving in the optical molasses experience the polarization gradients and are optically pumped by the molasses light to redistribute a population in their Zeeman sublevels of ground states. This effect gives another cooling mechanism that can cool atoms down below the Doppler limit, called "polarization gradient cooling, PGC".

There are two configurations to form the polarization gradient. The first one uses the counterpropagating laser beams of orthogonal linear polarizations to produce a local polarization that varies from linear to circular to orthogonal linear and to orthogonal circular with a spatial period of $\pi/2$. The second one uses the counterpropagating light beams of σ_- and σ_+ polarizations to form a linear polarization that rotates around the beam direction as shown in Figure 2.9. Corresponding to these two types of gradient, there are two different PGCs that can be realized [39].

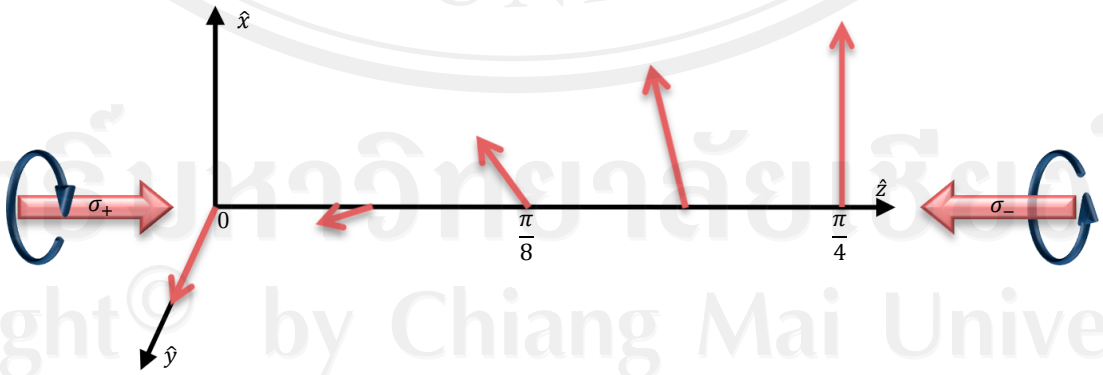

Figure 2.9. Polarization gradient field for the σ_--σ_+ configuration.

In this study, PGC with σ_- - σ_+ configuration was used because the polarizations of the cooling beams are the same as that use in the MOT. Let us consider a moving atom in this polarization gradient with speed v. The atom responds to the local polarization of light with an optical pumping time τ_p, characterizing the mean time that it is transferred by fluorescence cycle to the other sublevel. If the atom is moving slowly enough ($\tau_p \ll \frac{\lambda}{2v}$, where λ is a wave length of the light), the light will have enough time to optically pump the atom into a state that has an orientation corresponding to the local polarization. On the other hand, for the fast atom ($\tau_p \gg \frac{\lambda}{2v}$), the optical pumping rate is too slow to make the orientation. In this case, the atom will be cooled by the Doppler cooling only.

To understand this PGC mechanism, the simplest model explains the ground-state orientation by using the atoms having $J = 1$. If the atoms is at rest at $z = 0$ and we take the quantization axis along the local linear polarization axis which is $\hat{y}$ as seen in Figure 2.9. The atoms will be optically pumped to redistribute their populations of the magnetic substates. Due to the linear polarization, the most of them tend to be accumulated in the $m = 0$ sublevel and a smaller portion of them populate in the $m = +1$ and $m = -1$ sublevels equally. For the atoms moving in the same direction of the beams, they experience the rotation of the linear polarization and are optically pumped in order to follow it. However, the ground substate population of the moving atoms always lags behind the steady state distribution following the local field [39]. From this effect, the atoms traveling toward the σ_+ beam will populate the $m = +1$ state more than the $m = -1$ state and vice versa the $m = -1$ state is more populated for the atoms traveling in opposite direction.

This small imbalance in the distribution of the ground substate creates the large force to damp the atomic velocity. That is because the atoms with $m = +1$ have a higher probability to absorb the σ_+ photon than the σ_- photon (see the transition strength in Appendix A) and the most of them travel toward the σ_+ beam. Thus their motion will be damped by the radiative force of the σ_+ beam. For the atoms traveling toward the σ_- beam, they are optically pumped into the $m = -1$ state and then is slowed down by the radiative force of σ_- beam.

This PGC mechanism relies on the unbalance of the two radiative forces when the atom is moving due not to the Doppler shifts of two laser beams as in the Doppler cooling, but to an unbalance of the ground substate distribution because of the time lag of the atom orientation to follow the local field.

2.1.5 Sisyphus cooling

Another efficient cooling method called Sisyphus cooling is based on the stimulated emission [40]. Consider an atom moving in a spatially periodic potential created by a standing light wave. This causes an exchange between kinetic and potential energy of the atom. If the standing wave is formed by two counterpropagating light beams with frequency ω that is blue detuned δ from the atomic resonance. For a weak light intensity (saturation parameter $s \lesssim 1$), the beams produce heating of the atom because of the Doppler effect. By contrast, when the light intensity is high enough (saturation parameter $s \gg 1$), the beams produce a cooling mechanism due to the emission processes that are predominant over the Doppler heating.

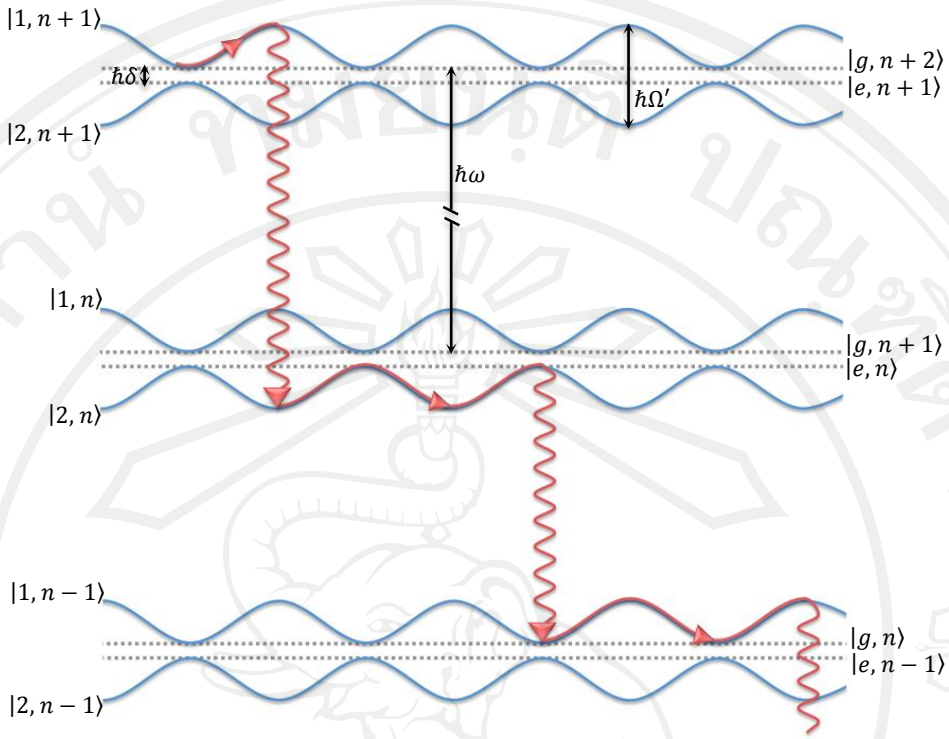

Figure 2.10. Sisyphus cooling processes in a strong standing wave. The blue lines represent the dressed atom energy levels, which are varied spatially due to the light intensity in the standing wave. The dotted lines represent the energy levels of the bare states. The red lines represent the atomic potential energy and where the spontaneous emissions occur.

A simple way to explain the atomic motion in the strong standing wave is using a dressed state picture as represented in Figure 2.10. The dressed energy levels are varied spatially following the light intensity (or the number of photons) in the standing wave. At a node position with the vanished intensity, the Rabi frequency Ω is equal to zero. Thus the coupling dressed states $|1, n+1\rangle$ and $|2, n+1\rangle$ coincide with the uncoupled states $|g, n+2\rangle$ and $|e, n+1\rangle$, respectively, where g and e represent the ground state and the excited state, respectively, and n is the light field quantum number as mentioned before Equation (2.10) in Section 2.1.3. Because the

light is blue detuned by δ, the energy level of $|g, n+2\rangle$ is higher than the level of $|e, n+1\rangle$ by $\hbar\delta$. At a position with the non-zero intensity, the dress state $|1, n+1\rangle$ start to have a nonzero coefficient of $|e, n+1\rangle$ and the state $|2, n+1\rangle$ also has a nonzero coefficient of $|g, n+2\rangle$ as well. In consequent the energy splitting is increased as $\hbar\Omega' = \hbar[\delta^2 + \Omega^2]^{1/2}$ written in Equation (2.11). This splitting is largest at the antinodes of the standing wave where the light intensity is highest.

Let us consider the atom having trajectory as shown in Figure 2.10. The atom in $|1, n+1\rangle$ travels in the periodic of energy level starting from the valley. It climbs up to the top of the potential hill where contains the largest coefficient of $|e, n+1\rangle$. Thus at this position, the atom has the maximum probability to spontaneously emit photon and decay into the lower dressed states $|1, n\rangle$ or $|2, n\rangle$ containing $|g, n+1\rangle$. If the atom decays into $|1, n\rangle$ where it is on the top of the hill, this will not change any thing from a mechanical point of view. By contrast, if the atom decays into the $|2, n\rangle$ level where it is in the valley again. In this case, the velocity of the atom will be decreased because its kinetic energy is converted to potential energy while climbing up to the top of the hill and then jumps to the bottom of another one by the spontaneous emission. Now the atom in $|2, n\rangle$ starts to climb up again to the top of the hill where the probability to decay is highest because of the equivalent of $|2, n\rangle$ and $|e, n\rangle$ at the nodes of the standing wave. Then the atom may decay to the valley of the lower level again as shown in the figure. Thus the atom seems to be always climbing the hills and losing its potential energy by spontaneously emitting photon. This process will repeat until the atom has too small kinetic energy to climb the next hill. This cooling process exhibits a picture similar to when Sisyphus in Greek

mythology tried to interminably push a huge rock up the hill; the reason why this cooling method is called the Sisyphus cooling.

2.2 Trap loss

For atoms in trap, the atom loss experiments have shown that the main loss mechanism is caused by the atomic collisions. To understand the trap loss, let us start with the rate of trap loss due to the collisions, which can be measured by observing the number of atoms in a trap N that changes by the rate

$$\frac{\mathrm{d}N}{\mathrm{d}t} = L - \gamma N - \beta \int_R \mathrm{d}^3 R' [n(R', t)]^2 \,, \tag{2.14}$$

where L is an atomic loading rate of the trap, γ is the decay rate constant, β is the loss rate constant, and $n(R, t)$ is the atomic cloud distribution [30].

The first term of this expression represents an atomic capture rate of the trap that depends on the trap parameters. The second term represents the decay mechanism due to the collision between trapped atoms and a thermal background gas. The last term represents the trap loss mechanism due to the collisions between two trapped atoms. To study the collisional loss, this section starts with discussion about the principle of the collision (Section 2.2.1), which can be induced by either red detuned light (Section 2.2.2) or blue detuned one (Section 2.2.3).

2.2.1 Light induced cold collisions

In the presence of light field, the inelastic collisions between cold atoms are induced. The theory of the collisions can be explained by using the quasimolecular picture, $|S+S\rangle$ and $|S+P\rangle$ states as represented in Figure 2.11. The $|S+S\rangle$ asymptote represents two ground state atoms that interact each other at an internuclear separation R. When the separation is of the order of optical wavelength, an attractive ground state potential is formed as

$$U_g(R) = \frac{C_6}{R^6} + \frac{C_8}{R^8} \ldots$$

$$\simeq \frac{C_6}{R^6}, R \gg 0\,, \tag{2.15}$$

where C_i is the coefficient resulting from the interaction, i is an integer number [41]. Here C_6 and C_8 are negative.

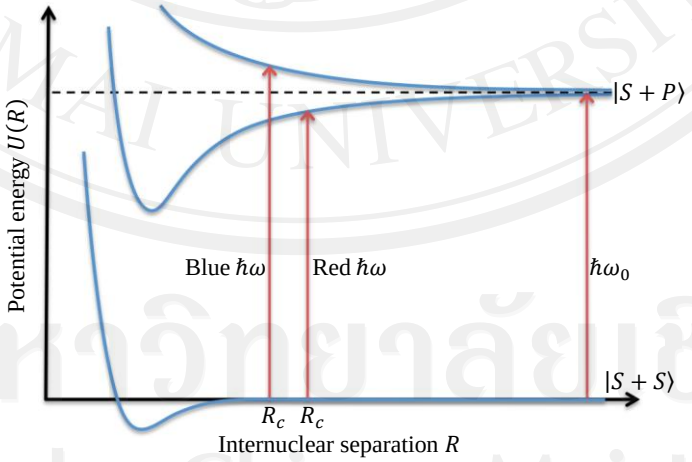

Figure 2.11. Schematic of the quasimolecular energy levels of $|\boldsymbol{S+S}\rangle$ and $|\boldsymbol{S+P}\rangle$ as a function of the internuclear separation $\boldsymbol{R}$.

The $|S+P\rangle$ asymptote represents one ground and one excited state atoms. The energy level of this state is above the ground state $|S+S\rangle$ by the atomic excitation energy $\hbar\omega_0$ and is shifted due to the interaction between two atoms. The excited potential correlating to the $|S+P\rangle$ can be calculated as

$$U_e(R) = \hbar\omega_0 + \frac{C_3}{R^3} + \frac{C_5}{R^5} \ldots$$

$$\simeq \hbar\omega_0 + \frac{C_3}{R^3}, R \gg 0. \tag{2.16}$$

From this equation if C_3 is negative, the energy level of $|S+P\rangle$ is shifted below the $\hbar\omega_0$ level. In contrast to the positive C_3, the energy level is shifted up as shown in Figure 2.11.

Let consider a collision between two ground state atoms in the light field $\hbar\omega$. Their probability of transition to $|S+P\rangle$ is highest at the Condon point R_C, where the separation between the two states is resonant with the field. For the detuning δ, R_C is given by

$$\hbar\delta = \frac{C_3}{R_C{}^3} \quad \text{or} \quad R_C = \left(\frac{C_3}{\hbar\delta}\right)^{1/3}. \tag{2.17}$$

In an inelastic collision process, if the atoms are in the red detuned light field, they will absorb a photon, transition to the lower $|S+P\rangle$, and approach to each other following the attractive potential curve. On the other hand, for the atoms in the blue detuned light field, they will be excited to the upper $|S+P\rangle$. In this repulsive potential the atoms will approach one another until they reach the turning point of the nuclear motion and start to separate from each other along the repulsive curve. In

either case, the atoms will decay back to $|S + S\rangle$ with the spontaneous decay and gain a certain amount of energy.

For collisions induced by the red detuned light, there are many studies about the collisions in MOTs leading to the traps loss. These studies are very important to getting more precise measurements of the MOT's properties. For the blue detuned light assisted collisions, this mechanism is used in preparing individual atom due to the controllability of the energy gained in the collision process. These two kinds of collisions will be explained in detail in the next sections.

2.2.2 Collisions in MOT

During loading MOT, the red detuned light is applied to cool and confine atoms. At the same time, the two cold atoms may absorb the light photon at the initial stage of a collsion. In this collision, the atoms gain more kinetic energy from an internal electronic energy leading to increase in the nuclear motion. If the velocity of the atoms is higher than the recapture ability of the MOT, the atoms will escape the trap. To explain this cold collision induced by the red-detunded light, a semiclassical Gallagher-Pritchard model (GP model) was proposed. The GP model has been improved by Juienned and Vigue called JV model.

Gallagher-Pritchard model

The GP model is the first theoretical approahes for cold collisions [42]. The model was propose to describe the trap loss mechanisms due to a fine-structure-changing

collision (FCC) and a radiative escape (RE). Figure 2.12 (a) and (b) show the two basic light-induced collisional trap loss processes which are FCC and RE respectively.

In the FCC mechanism (see Figure 2.12 (a)), two colliding atoms in the red detuned light field approach each other in the ground state $|S + S\rangle$. They may absorb the photon with energy $\hbar\omega$ and excite into $|S + P_{3/2}\rangle$ at the separation of R_0. In the excited state, they are accelerated along the separation R towards each other by the attractive potential. At a very small R, the potential becomes repulsive and then the atoms start to move apart again. However the $|S + P_{3/2}\rangle$ can be coupled to another fine structure state $|S + P_{1/2}\rangle$. Thus the atoms may change to $|S + P_{1/2}\rangle$ state and move far away from each other. Finally, the atoms spontaneously decay back to the ground state and emit photon with energy $\hbar\omega'$. The FCC process can be described by

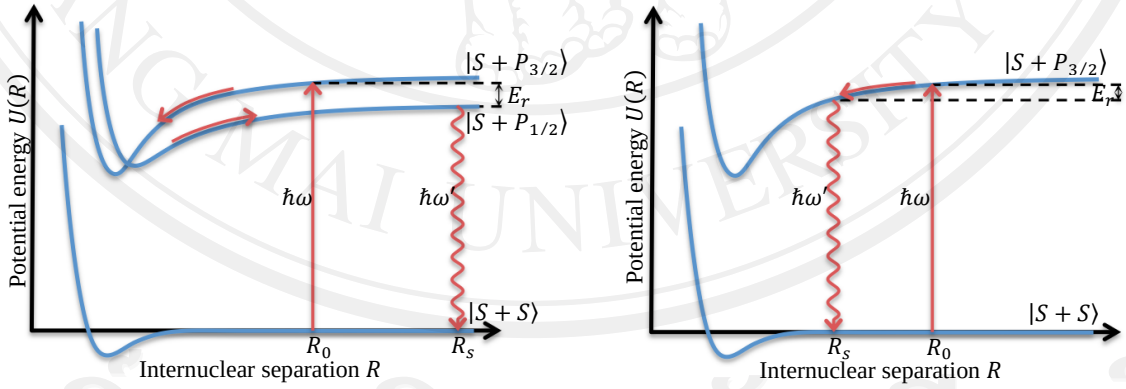

Figure 2.12. Schematic of the quasimolecular energy levels of $|\boldsymbol{S + S}\rangle$, $|\boldsymbol{S + P_{1/2}}\rangle$ and $|\boldsymbol{S + P_{3/2}}\rangle$ as a function of the internuclear separation $\boldsymbol{R}$. The two colliding atoms are in the light field with the frequency of $\boldsymbol{\omega}$, which is red detuned from the

atomic D2-line transition. Due to the light, the atom may undergo either the FCC (a) or RE (b) passage.

$$|S+\ S\rangle + \hbar\omega \longrightarrow |S + P_{3/2}\rangle \longrightarrow |S + P_{1/2}\rangle + \Delta E_{FS}$$

where ΔE_{FS} is the energy between fine structures, $|S + P_{3/2}\rangle$ and $|S + P_{1/2}\rangle$. In this FCC collision, the atoms gain kinetic energy equal to $E_r = \hbar(\omega - \omega') \approx \Delta E_{FS}$ where $h\delta \ll \Delta E_{FS}$.

In the RE mechanism (see Figure 2.12 (b)), after the absorbtion the atoms in $|S + P_{3/2}\rangle$ are accelerated towards each other. Then the atoms spontaneously emit photon with the energy of $\hbar\omega'$ and decay back to the ground state at the separation of R_s. In this case, the atoms gain released energy E_r, which is also equal to $\hbar(\omega - \omega')$. The RE process can be represented by

$$|S+\ S\rangle + \hbar\omega \longrightarrow |S + P_{3/2}\rangle \longrightarrow |S+\ S\rangle + \hbar\omega'.$$

The GP model begins with a stationary ground-state atom pair at internuclear separation R_0 in the light field and assumes that the excitation probability for the pair can be determined by an expression:

$$P_e(R_0) = \frac{\Omega^2}{[\delta(R_0)]^2 + (\Gamma_M/2)^2}, \tag{2.18}$$

where $\delta(R_0)$ is the local detuning which is $\omega - \left[U_e(R_0) - U_g(R_0)\right]/\hbar$. For this model, the ground-state energy level $U_g(R)$ is estimated to be zero at any R. This quasistatic approximation is reasonable if the collision processes is slow enough.

From this expression, the model allows the colliding pair to be excited at an off-resonant position ($R_0 \neq R_C$) and the bounds are limited by the molecular linewidth Γ_M.

After excitation, the two atoms on quasimolecular excited state $|S + P_{3/2}\rangle$ are accelerated by the attractive potential $U_e(R)$. Their relative radial velocity as a function of the separation then is

$$v(R) = \sqrt{\frac{2}{\mu}\{E_{k0} - [U_e(R) - U_e(R_0)]\}}, \tag{2.19}$$

where μ is the reduce mass, E is an initial relative kinetic energy of the atoms. A classical time that is required to travel form R_0 to R_s, is given by $t = \int_{R_0}^{R_s} \frac{\mathrm{d}R}{v(R)}$. Thus the probability that the quasimolecule survives in the excited state to the internuclear separation R_s is

$$S = exp(-\Gamma_M t)$$

$$= exp\left(-\Gamma_M \int_{R_0}^{R_s} \mathrm{d}R \left[\frac{2}{\mu}\{E_{k0} - [U_e(R) - U_e(R_0)]\}\right]^{-1/2}\right). \tag{2.20}$$

For calculation of S in this GP model, Gallagher and Pritchard ignored the initial kinetic energy E_{k0}, assumed Γ_M to be a constant $2\Gamma_A$ where Γ_A is an atomic linewidth and set $R_s = 0$. This survival probability of the GP model then is

$$S_{GP} = exp\left(-(\delta_\tau/\delta)^{5/6}\right), \tag{2.21}$$

where δ_τ is the detuning corresponding to $R_0 = R_\tau$ where $\tau = {\Gamma_M}^{-1} = \int_{R_\tau} \frac{\mathrm{d}R}{v(R)}$. If the excited quasimolecule can reach the coupled region between $|S + P_{3/2}\rangle$ and $|S +$

$P_{1/2}\rangle$ where the FCC occurs, it rapidly passes this region twice. A net total angular momentum J-changing probability (the quasimolecule undergoes the $|S + P_{1/2}\rangle$ channel), η_J, is equal to $2P_{LZ}(1 - P_{LZ})$ where P_{LZ} is the Landau-Zener single-transit curve-crossing probability (will be explained in the next subsection, Landau-Zener transition). If the quasimolecule oscillates through the crossing, the FCC probability is the sum of the probability of each repeated crossing [43],

$$P_{FCC} = \frac{\eta_J S_{GP}}{\left(1 - {S_{GP}}^2 + \eta_J {S_{GP}}^2\right)}. \tag{2.22}$$

The probability of radiative escape, P_{RE}, is obtained from integration similar to the FCC one. This GP model considers only the quasimolecule that transits in an inner R region where its released energy E_r is greater than an energy needed to achieve radiative escape in MOT. If the quasimolecule spends time $2t_E$ in this region before spontaneous decay, then the RE probability can be written as

$$P_{RE} = \frac{2t_E \Gamma_M S_{GP}}{\left(1 - {S_{GP}}^2 + \eta_J {S_{GP}}^2\right)}. \tag{2.23}$$

Julienne-Vigue model

Another model that improves the GP model was proposed that is called JV model [44]. The model was added a thermal averaging procedure, used the retarded molecular spontaneous emission decay rates $\Gamma_M(R)$ instead of constant value ($2\Gamma_A$), and employed realistic hyperfine molecular states by taking into account angular momentum quantum number dependence in the survival probability in an excited

state S. The JV model agrees well with the GP model when the JV model makes the same approximation as GP model.

In both GP and JP models, the atoms are determined to share the released energy from collision equally. In consequent, a high released energy leads to the trap loss of the both collisional partners.

Landau-Zener transition

In the coupling region, the atoms may move approach to each other through the region adiabatically following the dressed state level (solid lines). The atoms also have a potential to transition to another dressed state. This mechanism is called Landau-Zener (LZ) transition. The probability of LZ transition can be determine by [43],

$$P_{LZ} = \exp\left(-\frac{2\pi\hbar\Omega^2}{Dv}\right), \tag{2.24}$$

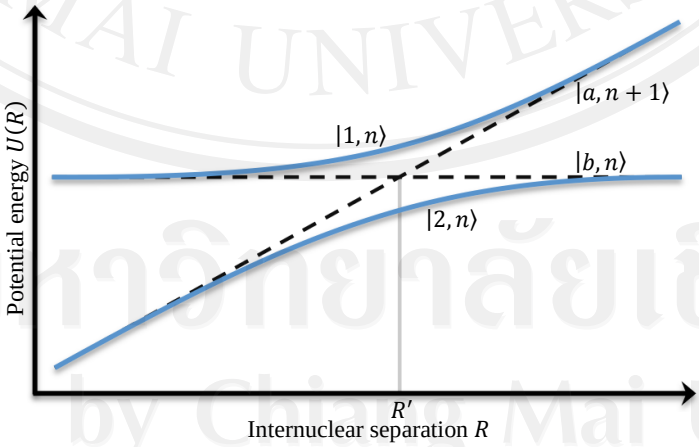

Figure 2.13. Schematic shows the energy levels of the dressed states $|\mathbf{1}, \boldsymbol{n}\rangle$ and $|\mathbf{2}, \boldsymbol{n}\rangle$ (solid lines) compared with the uncouple levels of the bare states $|\boldsymbol{a}, \boldsymbol{n}+\mathbf{1}\rangle$ and $|\boldsymbol{b}, \boldsymbol{n}\rangle$ (dashed lines) as a function of the internuclear separation.

where $D = \left|\frac{\mathrm{d}[U_e(R)-U_g(R)]}{\mathrm{d}R}\right|_{R'}$ is the slope of the difference potential energy at crossing point, R'. Then the probability that the atoms undergo the adiabatic passage [43], is

$$P_A = 1 - P_{LZ} = 1 - \exp\left(-\frac{2\pi\hbar\Omega^2}{Dv}\right). \tag{2.25}$$

Suppose that the atoms approach toward each other in the $|1, n\rangle$ dressed state. There are two pathways that the atoms will end up in $|2, n\rangle$ when they move apart each other. As the atoms pass this coupling region twice (when they are approaching and leaving each other), the atoms may undergo the adiabatic passage through the $|1, n\rangle$ level with the probability of P_A before they LZ transition into the $|2, n\rangle$ level with the probability of P_{LZ}. In the other way, the atoms may transition into the $|2, n\rangle$ level with the probability of P_{LZ} before undergo the adiabatic passage in the $|2, n\rangle$ level with the probability of P_A. In summary, the atoms that start in $|1, n\rangle$ have a probability to end up in $|2, n\rangle$ equal to $2P_{LZ}P_A$ or $2P_{LZ}(1 - P_{LZ})$.

2.2.3 Blue detuned light assisted collisions

In a presence of blue detuned light field, the light can prevent atoms from closely approaching each other. This process is known as "optical shielding" and can be described via a semiclassical picture as seen in Figure 2.14. The two approaching

atoms in $|S+S\rangle$ (as represented by grey arrow) are excited into $|S+P\rangle$ by absorbing the photon around the Condon point R_c.

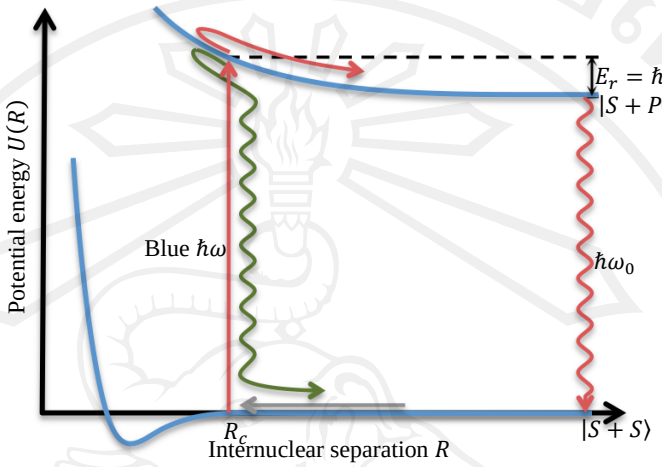

Figure 2.14. Schematic shows a model of collisional process induced by a blue detuned light with the frequency of $\boldsymbol{\omega}$. The quasimolecular energy levels of $|\boldsymbol{S+S}\rangle$ and $|\boldsymbol{S+P}\rangle$ as a function of the internuclear separation $\boldsymbol{R}$ are indicated by the solid blue lines. Grey arrow represents two atoms that approach each other in their ground state. Red and green arrows represent the inelastic and elastic collision between the atoms induced by blue detuned light respectively.

In the excited state, the closer distance between atoms is suppressed due to the repulsive potential. As a result, they move apart and exit either in $|S+P\rangle$ (as represented by red arrow) or in $|S+S\rangle$ (as represented by green arrow). In the case of an exit in $|S+S\rangle$, the released energy for the atoms is equal to zero and the collision then becomes elastic. An inelastic collision occurs when the atoms exit on $|S+P\rangle$. They travel following the repulsive potential; decay to $|S+S\rangle$; and gain the released energy that equals to $\hbar\delta$. That means the energy released from this inelastic collisions could be controlled through the detuning of the light.